Development of a Distinct Later Phase Associated with Shallow, Outer-rise Earthquakes along the Japan Trench - FDM Simulation using the Earth Simulator

Project Representative
Takashi Furumura — Center for Integrated Disaster Information Research, Interfaculty Initiative in Information Studies, The University of Tokyo / Earthquake Research Institute, The University of Tokyo

Authors
Shinako Noguchi — Central Research Institute of Electric Power Industry
Takuto Maeda — Earthquake Research Institute, The University of Tokyo
Takashi Furumura — Earthquake Research Institute, The University of Tokyo
Center for Integrated Disaster Information Research, Interfaculty Initiative in Information Studies, The University of Tokyo

We investigated the development of a distinct later phase observed at stations near the Japan Trench associated with shallow, outer-rise earthquakes off the coast of Sanriku, northern Japan based on the FDM simulations of seismic wave propagation using a heterogeneous structural model of the Japan Trench subduction zone. Snapshots of seismic wave propagation obtained through these simulations clearly demonstrate the complicated seismic wavefield constructed by a coupling of the ocean acoustic waves and the Rayleigh waves propagating within seawater and below the sea bottom by multiple reflections associated with shallow subduction zone earthquakes. We demonstrated that the conversion to the Rayleigh wave from the coupled ocean acoustic waves and the Rayleigh wave as they propagate upward along the slope of seafloor near the coast is the primary cause of the arrival of the distinct later phase at the station near the coast. Through a sequence of simulations using different structural models of the Japan Trench subduction zone, we determined that the thick layer of seawater along the trench is the major cause of the distinct later phase.

Keywords: Guided wave, Rayleigh wave, Scholte wave, ocean acoustic wave, outer-rise earthquake

1. Introduction

A large-amplitude, long-period (T = 15 s) Rayleigh wave packet is observed at F-net broadband stations (Okada et al., 2004)[1] located onshore and on islands of the Pacific Ocean from shallow, outer-rise earthquakes occurring off the coast of Sanriku, northern Japan. The amplitude of the later Rayleigh wave is very large, almost as large as the S wave, which is characterized as a predominant feature emerging from long S wave coda.

Such later Rayleigh wave packets can be observed in a special combination of source and observation stations and when the ray path travels through the deep Japan Trench. Therefore, this phase is expected to be generated or converted during propagation along the Japan Trench with strong lateral heterogeneities in the subduction zone structure. Since the structure of the Japan Trench is formed by the subducting high-wavespeed Pacific Plate, steeply dipping seafloor from land to offshore, thick low-wavespeed sediments covering the seafloor and the subducting plate, and deep seawater, the combined effect of each heterogeneity is expected to modify seismic wave propagation dramatically.

Similar observations have been reported by Nakanishi et al. (1992)[2] from shallow earthquakes occurring near the Kuril Islands above the Kuril Trench and for stations in Hokkaido, northern Japan. Yomogida et al. (2002)[3] demonstrated through a ray-theory-based simulation that a thick column of seawater parallel to the trench axis acts a waveguide for the Rayleigh wave during shallow earthquakes occurring near the trench. Considering the similarity in the characteristics of the observed phase and the source-to-station geometry, the observations of the present study at the Japan Trench may have the same origin.

The purpose of this study is to investigate the cause of such phenomena based on the numerical simulation of seismic wave propagation. In the following section, we first analyze three-component broadband seismograms of the F-net broadband network across Japan in order to examine the characteristics of a peculiar seismic phase more clearly. We then perform computer simulations of seismic wave propagation using the detailed subsurface structure of the Japan Trench subduction zone using a two-dimensional finite-difference method (FDM). Through

these simulations, we examine the contribution of the seawater layer on the development of the peculiar later phase.

2. Observation of the Trench-converted Rayleigh Wave

A large, Mw 7.0, earthquake occurred off the coast of Sanriku, northern Japan on 14 November 2005 at a depth of 18 km, which is categorized as an outer-rise earthquake occurring within the subducting plate before entering the subduction zone (Fig. 1, Table 1).

Seismograms from the 2005 Mw7.0 Sanriku earthquake were well recorded over a wide portion of the Japanese Islands, clearly demonstrating the propagation of the P and S waves, as well as the propagation of a large Rayleigh wave that developed as a result of the shallow earthquake. Moreover, an anomalous later arrival appears in the seismogram of the F-net broadband station of AOGF, at the Island of Aogashima. The three-component displacement record at AOGF is shown in Fig. 2. This record exhibits large amplitudes and longer-period signals in three-component motions. This peculiar signal (referred to hereinafter as the X phase) has prolonged long wave trains with a duration of approximately 130 s. The X phase is identified in three-component motions and has a large vertical (UD) component with the amplitude that is comparable to those of the Rayleigh wave and the S wave in horizontal motion. Assuming the epicentral distance from the source to AOGF is approximately 800 km, the apparent velocity of the X phase can be roughly estimated to be 1.2 km/s, which is too slow to be from surface waves propagating directly from the source.

The X phase exhibits a monochromatic dominant period of approximately T = 15 s, which is much longer than that of the Rayleigh wave (T = 10 s) observed at an earlier time. The particle motion of the X phase shown in Fig. 3 exhibits a linear polarization in which the long axis of the trajectory is approximately in the direction of the hypocenter, but deviates by approximately 20 degrees eastward from the great circle path. In addition, the particle motion of the X phase is characterized

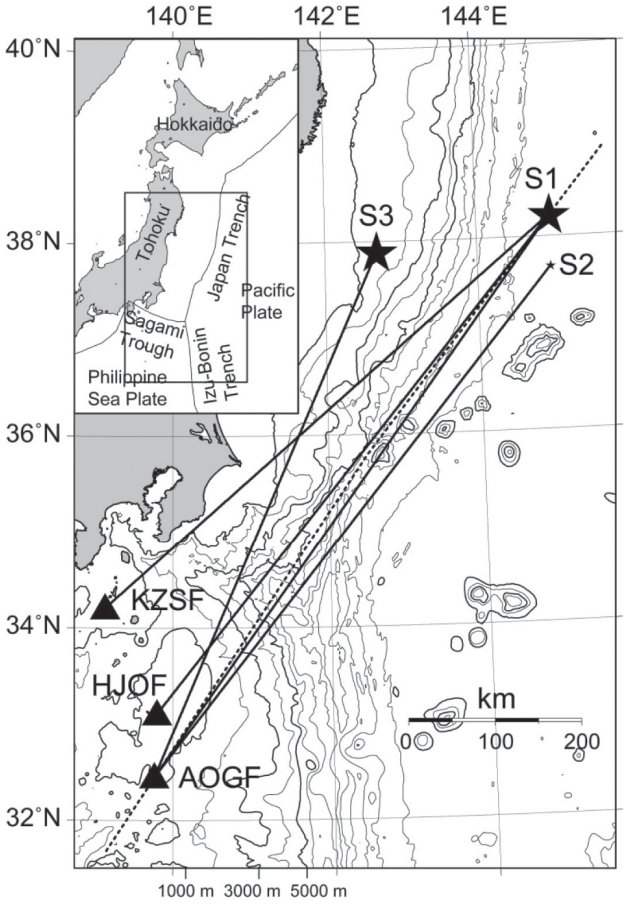

Fig. 1 Map of the source (stars: S1-S3) and the F-net broadband stations (KZSF, HJOF, and AOGF: triangles) used in the present study. The lines connecting the epicenters and stations are the expected propagation paths of seismic waves along the great circle path. The dashed line connecting S1 to AOGF indicates the profile for 2D FDM simulation shown in Fig. 6.

Table 1 List of earthquakes and source parameters.

	Origin time (UTC)	Longitude	Latitude	Depth (km)	Mw Type
S1	2005/11/14, 21:38	144.90	38.11	18	7 outer-rise
S2	2005/11/01, 16:09	144.96	37.69	16	4.9 outer-rise
S3	2003/10/31, 01:06	142.62	37.81	15	7 interplate

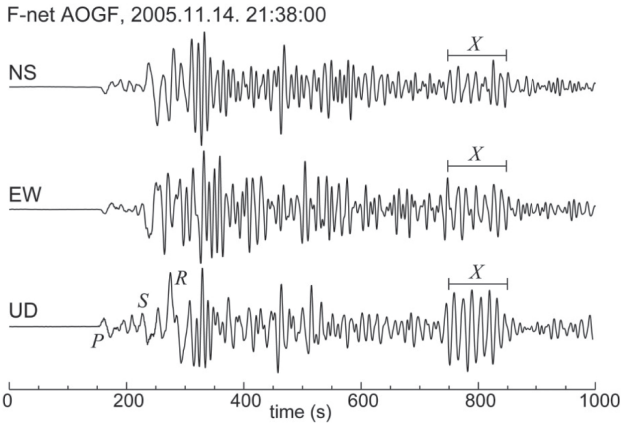

Fig. 2 Three-component displacement waveforms recorded at the AOGF station during the 2005 earthquake off the coast of Sanriku (S1 in Fig. 1). Each trace is normalized by its maximum amplitude. The arrival of the P wave, the S wave, and the Rayleigh wave (R) are indicated in the figure. The anomalous later phase (X phase) is indicated by X.

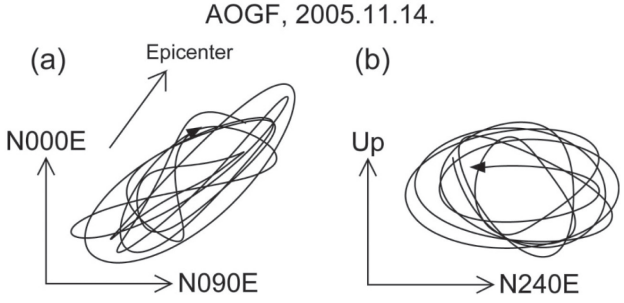

Fig. 3 Particle motions of the X phase in (a) the horizontal plane and in (b) the vertical plane for the AOGF station. The particle motion is calculated in the time window from 750 to 800 s in Fig. 2.

by a retrograde motion in the vertical plane. These observations indicate that the X phase is the Rayleigh wave developed by conversion from the S wave or the Rayleigh wave somewhere during the propagation path from the source off the coast of Sanriku to AOGF, but not above the source area.

We found a similar phase at F-net HJOF, approximately 30 km north of AOGF. However, no peculiar signal was observed at KZSF on the Island of Kouzu, 90 km further north (Fig. 1 and Fig. 4). Thus, the observation area of the X phase is extremely limited, even considering the dense F-net network, indicating that this signal is not developed near the source area, but instead is probably developed by the heterogeneous structure near the AOGF. For the other earthquakes nearby, we analyzed the waveform of shallow ($h < 20$ km) and relatively large ($M > 4.5$) earthquakes in order to investigate the observation conditions of the X phase. Fig. 5 shows the vertical component ground motion for other earthquakes, namely, an outer-rise Mw 4.9 event at a depth of 16 km (mark S2 in Fig. 1) and an Mw 7.0 inter-plate event at a depth of 15 km occurring near the coast across the trench (mark S3 in Fig. 1). The source parameters of these events are listed in Table 1. The S2 event exhibits a similar type of phase in the record of the AOGF. However, the S3 event does not produce such signals at all stations. An examination of the ray path for three events and for three F-net stations (Fig. 1) confirms that the ray path along which the X phase is observed is aligned over the Japan Trench axis. On the other hand the ray paths from S1 to KZSF and from S3 to AOGF, where no X phase is observed, are approximately aligned outside the trench. These results strongly suggest that the X phase is produced by a thick seawater column along the Japan Trench, as reported by Yomogida et al. (2002)[3] for Kuril Trench events.

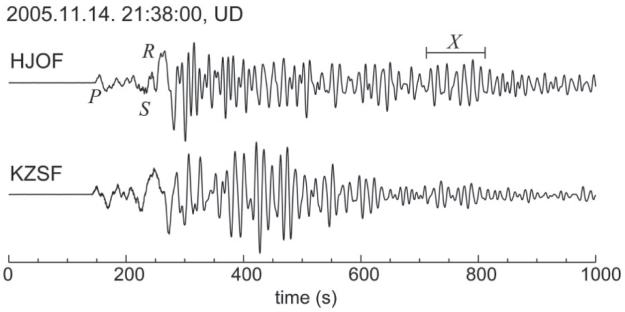

Fig. 4 Comparison of vertical component displacement waveforms observed at neighboring stations around AOGF during the 2005 earthquake off the coast of Sanriku. Each waveform is normalized by the maximum amplitude.

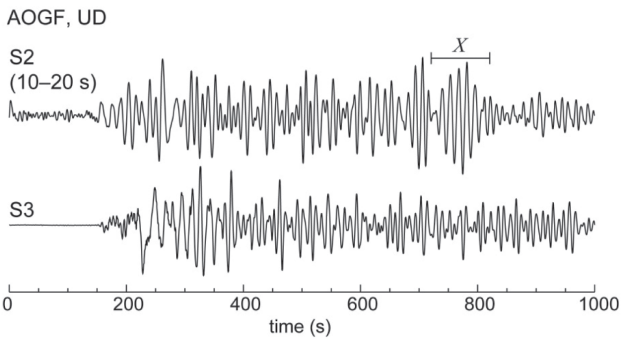

Fig. 5 Comparison of vertical component displacement waveforms at AOGF for three earthquakes (S1–S3, see Fig. 1). A band-pass filter with a pass-band period of from 10 to 20 s is applied to the S2 waveform to cut large long-period noise, and the other is unfiltered.

3. Numerical Simulation of the Trench-Converted Rayleigh Wave

In order to examine the process in which the peculiar X phase is developed in the Japan Trench, we perform a two-dimensional FDM simulation of seismic wave propagation using heterogeneous structure models of the cross section of the Japan Trench considering the case of off-Sanriku earthquake and AOGF mentioned above. Snapshots of the seismic wave propagation and synthetic seismograms, which are obtained directly by FDM simulation, are used to clarify in detail the complicated seismic wavefield in the heterogeneous structure and the development process of the X phase.

3.1 Simulation model

The simulation model covers a zone of 1000 km by 200 km from the hypocenter off the coast of Sanriku to the F-net AOGF station across the Japan Trench (Fig. 6 and the dashed line in Fig. 1). The 2D profile of the simulation model is constructed along a line that twists slightly from the great circle path from source to station in order to avoid cutting through the seamounts above the ray path. The seamount is less than 10 km, which is too small to have a strong effect on the propagation of the X phase of longer wavelength (approximately 18 km). However, the effect may be overestimated in the present 2D simulation because 2D simulation assumes that the structure and wavefield continue infinitely in the direction perpendicular to the 2D model.

The subduction zone structure across the Japan Trench shown in Fig. 6 is obtained from the seafloor topography data J-EGG500 compiled by the Japan Oceanographic Data Center, the subsurface structure by J-SHIS by National Research Institute for Earth Science and Disaster Prevention, and the depth of the subducting plates obtained from the Special Project for Earthquake Disaster Mitigation in Urban Areas. The physical

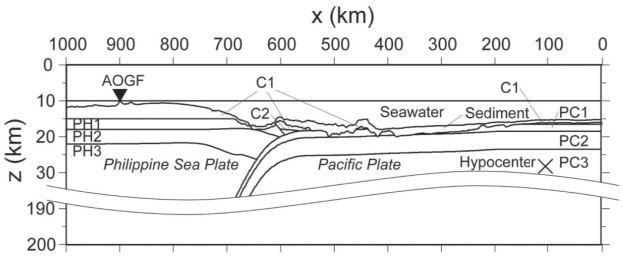

Fig. 6 Model of a 2D FDM simulation along the profile from S1 to AOGF (dashed line in Fig. 1). The physical parameters of each medium are shown in Table 2.

Table 2 Physical parameters for the 2D FDM simulation model.

	Density (10^3 kg/m^3)	Vp (km/s)	Vs (km/s)	Qp	Qs
Seawater	1.00	1.50	0.00	-	-
Sediment	1.80	3.50	1.00	90	50
C1	2.70	6.00	3.53	680	400
C2	2.80	6.70	3.94	680	400
PH1	2.40	5.00	2.90	340	200
PH2	2.90	6.80	4.00	510	300
PH3	3.20	8.00	4.70	850	500
PC1	2.60	5.40	2.70	340	200
PC2	2.80	6.50	3.40	510	300
PC3	3.40	8.10	4.60	850	500

parameters of the P- and S-wave speeds, the density, and the anelastic attenuation coefficients (Qp and Qs) for each layer are listed in Table 2. The simulation model shows a laterally heterogeneous structure with a large impedance contrast between the high-wavespeed subducting plate (Vs = 3 km/s) and the overlying thick (1 to 4 km), low-wavespeed sediments (Vs = 1 km/s) and the thick layer of seawater above the subduction zone, which might produce strong conversion and scattering of the seismic wavefield.

A seismic double-couple source of normal fault is located 18 km below sea surface (approximately 12 km below the seafloor), which radiates seismic waves with a Hermann (1984)[4] bell-type source-time function. The radiation pattern of the source is set considering the realistic mechanism which has the strike angle of 181 degrees, dip of 43 degrees and strike -104 degrees determined by Harvard Global CMT Catalogue. Considering the width of source fault model derived by Hino et al. (2009)[5], we set the source time duration of 10 s.

The seismic wave propagation is evaluated by calculating the equations of motion and constitutive equations based on a fourth-order staggered-grid FDM. The anelastic attenuation for the P and S waves (Qp and Qs) is modeled in the FDM simulation based on the memory variable technique (Hestholm, 1999 [6]). A perfectly matching layer (PML) absorbing boundary condition (Chew and Liu, 1996 [7]) is applied in the 20 grid points surrounding the model in order to suppress artificial reflections from model boundaries.

In this simulation, we introduced an accurate fluid-solid boundary condition developed by Okamoto and Takenaka (2005)[8] at the sea bottom and the sea surface, because such fluid/solid and fluid/air boundaries might be crucial in the development of the Rayleigh wave due to the coupling of the P and SV waves at the boundary and in the propagation and scattering of the Rayleigh wave over irregular sea topography.

The FDM simulation model is discretized with a grid interval of 1 km in the horizontal (x) direction and with a finer grid of 0.2 km in the vertical (z) direction in order to model the heterogeneous structure more effectively. The minimum S-wave velocity in the sediment (Vs = 1 km/s) and the relatively small gridding (dx = 1 km) allows seismic wave propagation with periods longer than T > 8 s with a sampling of eight grid points per minimum wavelength. By 200,000 time-step calculations with a time increment of dt = 0.005 s, we simulated seismic wave propagation for 1000 s.

3.2 Simulation Results

The results of the FDM simulation are shown in Fig. 7 along with snapshots of the seismic wave propagation and a synthetic seismogram of vertical component ground motion of each distance recorded at the sea bottom or on land. In the snapshots, the P and the SV wavefields are separated by taking the divergence and the rotation of the 2D wavefield, respectively. The contribution of the P wave is shown in red in the elastic media and blue in the water, and the contribution of the SV wave is shown in green. Such visualization of the P and SV waves is very useful in order to identify the characteristics of the seismic phases and to clarify the coupling and conversion between P and SV waves at model boundaries.

The sequence of snapshots indicates that the propagation of P and S waves occurred at relatively faster speeds below sea bottom and that the ocean acoustic waves propagated in seawater by multiple reverberations. The amplitude of the Rayleigh wave developed at the sea bottom is very large due to the shallow, large earthquake. As the Rayleigh waves propagate along the sea bottom with a relatively slow wave speed, a long, dispersed wave train gradually develops. In this model, the dispersion of the Rayleigh waves is striking when propagation in the subduction zone due to very large velocity and that in the low-velocity (Vs = 1 km/s) sedimentary layer and the high-velocity oceanic crust (Vs = 2.4 km/s) are compared. The dispersed Rayleigh wave extends more than 300 km, as indicated by the synthetic seismograms with a long-time duration of ground motions of more than 200 s following the S wave. In addition, a group of water acoustic waves propagating in the deep (approximately 6 km) sea is revealed by multiple reflections between the sea surface and the sea bottom, which develop long wave trains having slow propagation speeds of approximately 1.1 to 3.2 km/s. The amplitude of the water acoustic wave developed by radiation of the P wave from the shallow earthquake is very strong, and, moreover, the attenuation of the water acoustic waves is very weak due to the very small anelastic attenuation for the P wave (high Qp) in water. The sequence of snapshots indicates that coupling of the Rayleigh wave and the water acoustic wave occurs at the sea bottom, producing a long-period, monochromatic waveform with a period of approximately T = 15 s. Such a coupled wave of the Rayleigh wave and the water acoustic wave is often referred to as the Scholte wave, a kind of Stoneley wave, which is often observed in geophysical experiments in oceanic area (e.g., Essen et al., 1998 [9], Kugler et al., 2007 [10]). The Scholte wave is

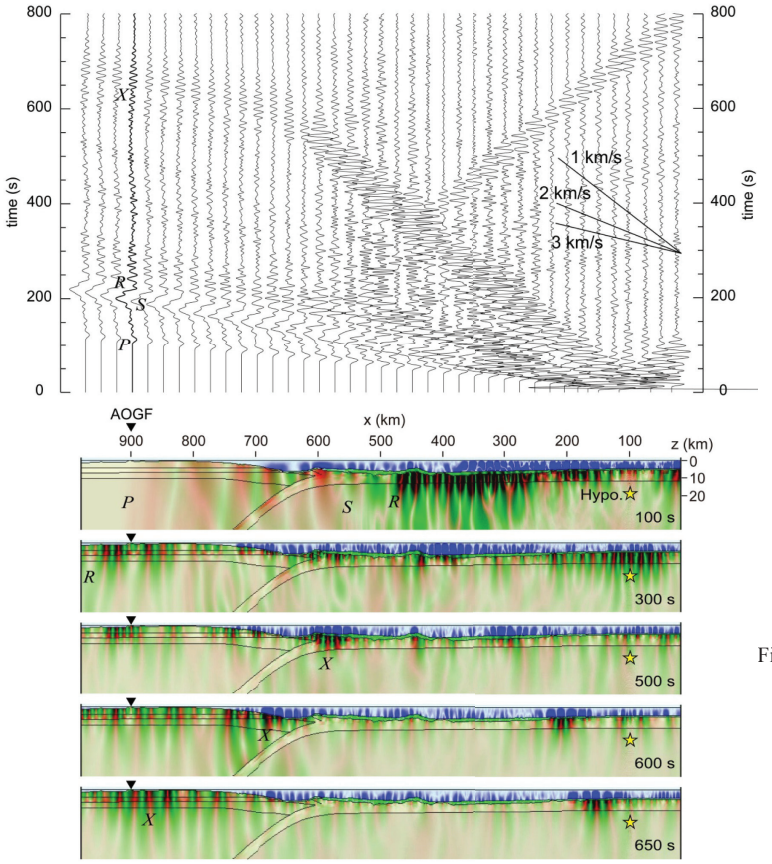

Fig. 7 Snapshots of seismic wave propagation at each time step from the start of the earthquake. Green and red represents P and S waves, respectively, and blue represents water acoustic waves. Major phases such as P, S, and Rayleigh waves and the X phase are indicated. A synthetic seismogram of the vertical component ground motion is shown at the top.

also known as a tube wave observed during seismic experiments in a fluid-filled borehole (e.g. Henriet et al., 1983 [11]). The tube wave shows much shorter period less than 0.1 or 0.01 s.

In the snapshots at later times (t = 600 s) the coupled Rayleigh wave/water acoustic wave propagating upward along the steeply uplifting seafloor sloop (at a distance of 600 to 800 km from the hypocenter) are found to be converted to the Rayleigh wave (denoted by R in the snapshots). Then, the converted Rayleigh wave propagating into the inland acquires large amplitude, which is comparable to the direct S wave, and propagates at a faster speed, which can be observed at AOGF stations at a distance of 900 km as a distinct phase. The synthetic seismograms of the vertical and radial component ground motions at AOGF obtained from the present simulation are shown in Fig. 8, demonstrating a large, monochromatic later wave packet with a duration of approximately 100 s and a dominant period of T = 15 s. The characteristics of the simulated signal explain very clearly the observed feature of the X phase at AOGF from the 2005 earthquake off the coast of Sanriku (Fig. 2). The retrograde particle motion of the X phase shown in Fig. 8(b) obtained from the present simulation also agrees very well with the observation (Fig. 3).

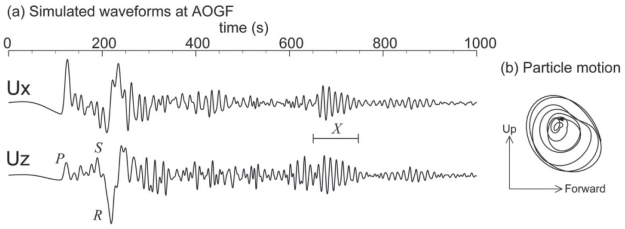

Fig. 8 Simulated displacement waveforms at AOGF with vertical and horizontal (radial) motions and particle motion in the vertical plane.

3.3 Effect of Seawater

We then conduct an additional simulation using a different structural model. In this simulation, we construct a simplified structure of flattened topography from the actual heterogeneous structure of the Japan Trench subduction zone in order to increase the visibility of the wavefield change as the model changes (Fig. 9).

We examine the effect of the thick layer of seawater covering the Japan Trench on the development of the X phase at AOGF. Figure 10 compares snapshots of the seismic wavefield and the synthetic seismograms of the vertical-component ground motion at AOGF obtained from the simulations using different sea depth models of h = 0, 3000, 6000, and 9000 m. Note that, as shown in Fig. 10, the inclination angle of the seafloor slope also changes with sea depth.

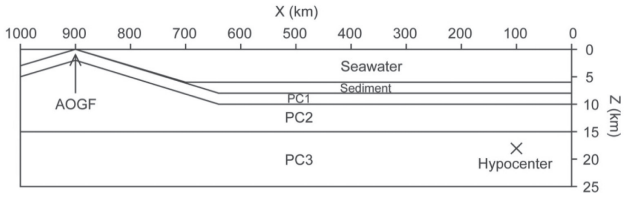

Fig. 9 Simplified model for the 2D FDM simulation of the X phase. The physical parameter of the each layer is shown in Table 2.

The results of the simulations reveal that the shape of the Rayleigh wave and the X phase change very dramatically with increasing sea depth from 0 to 9000 m, although the shape of the direct P and S waves is unchanged. The X phase gradually separates from the preceding Rayleigh waves. In addition, the propagation speed of the X phase increases as the thickness of seawater increases. Moreover, the X phase is confirmed not to develop in the absence of seawater. This result supports our interpretation that the X phase is a converted wave from the propagating coupled water acoustic waves and the Rayleigh wave, rather than simply originating the Rayleigh wave propagating along the sea bottom.

4. Discussion and Conclusion

In the present paper we investigated the cause of the distinct later arrival of the Rayleigh wave, referred to as the X phase, associated with shallow, outer-rise earthquakes observed at some coastal stations by 2D FDM simulations of seismic wave propagation using a heterogeneous structural model cutting through the Japan Trench subduction zone.

The snapshots of the seismic wave propagation obtained by the simulation reveal very clearly the complicated seismic wavefield of the ocean acoustic waves and the Rayleigh waves propagating in the sea by multiple reflections and along the sea bottom. The snapshots reveal that a strong coupling and mutual conversion occur between the ocean acoustic waves and the Rayleigh waves at the sea bottom, which produces a large and dispersed long-wave train of the Rayleigh wave as the propagation distance increases. As the coupled ocean acoustic waves and the Rayleigh wave approaching the coast, they are converted to the Rayleigh wave at the slope of the sea bottom and are observed at onshore seismic stations to have large amplitude. The X phase observed at AOGF during the outer-rise events off the coast of Sanriku was developed in such manner. The explanation of the developing process of the X phase presented herein is somewhat resembles to the results of Yomogida et al. (2002)[3], who explained that the thick layer of seawater in the trench is very important for guiding seismic waves over long distances and at low wave speed based on the ray-theory-based simulation. The synthetic seismogram of the AOGF station obtained by FDM simulation using the structural model of the Japan Trench succeeded in demonstrating the major characteristics of the observed X phase, such as the arrival time, the particle motion, the relative strength compared with the S wave, and the dominant period of the X phase. We also confirmed through a set of simulations that the shape of the X phase is sensitive to the seawater depth, although it does not modify the waveforms of direct P and S waves or the Rayleigh waves.

Most current ground motion simulations for subduction zone earthquakes use 2D and 3D structural models, in which the existence of seawater is not taken into account. This is due

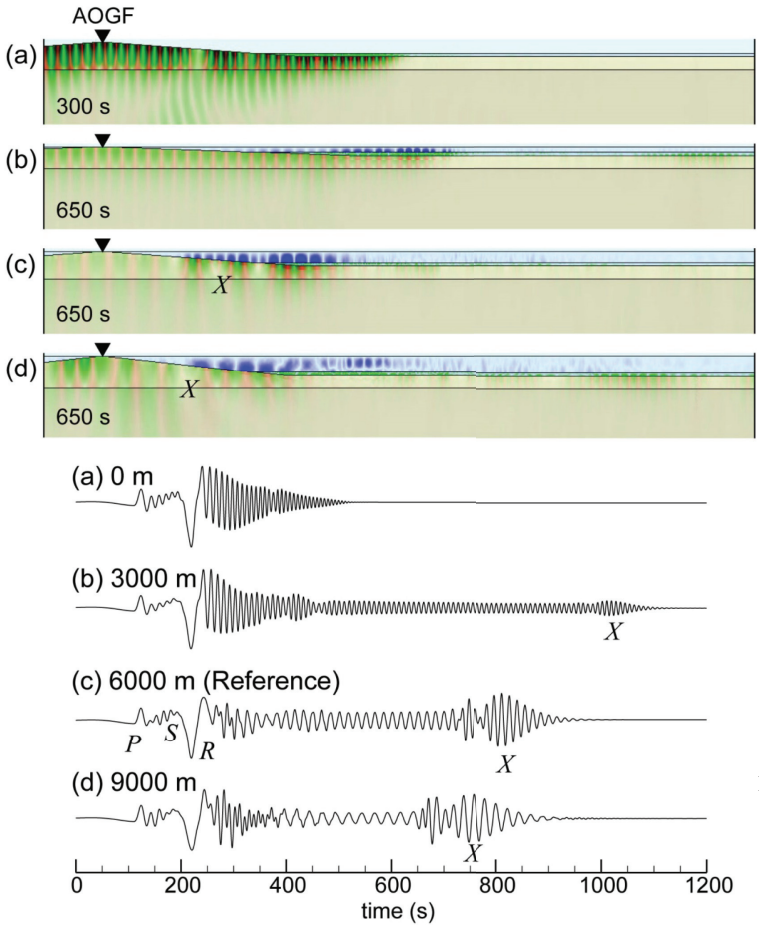

Fig. 10 Comparison of the vertical component displacement waveform at AOGF obtained by the FDM simulation considering the change in the waveform with varying sea depth from (a) 0 m, (b) 3000 m, (c) 6000 m, and (d) 9000 m.

primarily to increasing computational cost when including a low-wavespeed (Vp = 1.5 km/s) water column in the simulation model and the numerical stability problem associated with the low-wavespeed layers. However, the results of the present study emphasize the importance of the water layer on the propagation of the Rayleigh wave when examining relatively short-period signals of less than approximately T = 10 to 15 s, as has been discussed extensively by numerous researchers, including Shapiro et al. (2000)[12], Hatayama (2004)[13], Furumura et al. (2008)[14], and Petukhin et al. (2010)[15]. The simulation of the present study was restricted to the 2D case, but the effect of water layers with a laterally heterogeneous subsurface structure of the subduction zone should be more crucial in 3D.

Acknowledgements

We used the waveform record of the F-net broadband network operated by the National Research Institute for Earth Science and Disaster Prevention (NIED), Japan. We also acknowledge to NIED and Japan Oceanographic Data Center, Japan for providing subsurface structure and seafloor topography data, respectively. The computations were conducted on the Earth Simulator at Japan Agency for Marine-Earth Science and Technology (JAMSTEC). The present study was supported through the 'Integrated Predictive Simulation System for Earthquake and Tsunami Disaster' project of CREST, which funded by the Japan Science and Technology Agency. This study was published as the following paper: S. Noguchi, T. Maeda, and T. Furumura, "FDM simulation of an anomalous later phase from the Japan Trench subduction zone earthquakes", Pure Appl. Geophys., 170(1-2), 95-108, doi:10.1007/s00024-011-0412-1, 2013.

References

[1] Y. Okada, K. Kasahara, S. Hori, K. Obara, S. Sekiguchi, H. Fujiwara, and A. Yamamoto, "Recent progress of seismic observation networks in Japan – Hi-net, F-net, K-NET and KiK-net –", Earth Planets Space, vol.56, pp.xv-xxviii, 2004.

[2] I. Nakanishi, "Rayleigh waves guided by sea-trench topography", Geophy. Res. Lett., vol.19, pp.2385-2388, 1992.

[3] K. Yomogida, R. Okuyama, and I. Nakanishi, "Anomalous Rayleigh-wave propagation along oceanic trench", Stud. Geophys. Geod., vol.46, pp.691-710, 2002.

[4] R. B. Herrmann, "SH-wave generation by dislocation sources – a numerical study", Bull. Seism. Soc. Am., vol.69, pp.1-15, 1979.

[5] R. Hino, R. Azuma, Y. Ito, Y. Yamamoto, K. Suzuki, H. Tsushima, S. Suzuki, M. Miyashita, T. Tomori, M. Arizono, and G. Tange, "Insight into complex rupturing of the immature bending normal fault in the outer slope of the Japan Trench from aftershocks of the 2005 Sanriku earthquake (Mw = 7.0) located by ocean bottom seismometry", Geochem. Geophys. Geosyst., vol.10, Q07O18, doi:10.1029/2009GC002415, 2009.

[6] S. O. Hestholm, "Three-dimensional finite difference viscoelastic wave modeling including surface topography", Geophys. J. Int., vol.139, pp.852–878, 1999.

[7] W. C. Chew and Q. Liu, "Perfectly matched layers for elastodynamics: a new absorbing boundary condition", J. Comput. Acoust., vol.4, pp.341-359, 1996.

[8] T. Okamoto and H. Takenaka, "Fluid-solid boundary implementation in the velocity-stress finite-difference method", Zisin 2, vol.57, pp.355-364, 2005 (in Japanese with English abstract).

[9] H. -H. Essen, I. Grevemeyer, R. Herber, and W. Weigel, "Shear-wave velocity in marine sediments on young oceanic crust: constraints from dispersion analysis of Scholte wave", Geaphys. J. Int., vol.132, pp.227-234, 1998.

[10] S. Kugler, T. Bohlen, T. Forbriger, S. Bussat, and G. Klein, "Scholte-wave tomography for shallow-water marine sediments", Geophys. J. Int., vol.168, pp.551-570, 2007.

[11] J. P. Henriet, J. Schittekat, and Ph. Heldens, "Borehole seismic profiling and tube wave applications in a dam site investigation", Geophys. Prospect., vol.31, pp.72-86, 1983.

[12] N. M. Shapiro, K. B. Olsen, and S. K. Singh, "Wave-guide effects in subduction zones: evidence from three-dimensional modeling", Geophys. Res. Lett., vol.27, pp.433-436, 2000.

[13] K. Hatayama, "Theoretical evaluation of effects of sea on seismic ground motion", Proc. 13th WCEE, No.3229, Vancouver, Canada, 2004.

[14] T. Furumura, T. Hayakawa, M. Nakamura, K. Koketsu, and T. Baba, "Development of long-period ground motions from the Nankai Trough, Japan, earthquakes: observations and computer simulation of the 1944 Tonankai (Mw 8.1) and the 2004 SE off-Kii Peninsula (Mw 7.4) earthquakes", Pure Appl. Geophys., vol.165, pp.585-607, doi: 10.1007/s00024-008-0318-8, 2008.

[15] A. Petukhin, T. Iwata, and T. Kagawa, "Study on the effect of the oceanic water layer on strong ground motion simulations", Earth Planets Space, vol.62, pp.621-630, 2010.

海溝沿いの地震の際の特異な後続相についての地球シミュレータによる波動伝播シミュレーション

プロジェクト責任者
古村　孝志　　東京大学　大学院情報学環総合防災情報研究センター
　　東京大学　地震研究所
著者
野口　科子　　電力中央研究所
前田　拓人　　東京大学　地震研究所
古村　孝志　　東京大学　地震研究所
　　東京大学　大学院情報学環総合防災情報研究センター

海溝沿いの浅いアウターライズ地震の際に観測された特異な後続相について、海水の影響を考慮した差分法による波動伝播シミュレーションを行い、その結果から後続相の生成・伝播のメカニズムを推定した。シミュレーションの結果、海溝付近の直下で起きた地震により、海底の固体 - 液体境界面で境界波が生成され、海溝沿いの深海底を非常にゆっくりと伝播する様子が再現された。この波が、深海底を数百 km 伝播する間に S 波やレイリー波の主位相から数百秒遅れ、その後、陸域に至る海底斜面でレイリー波に変換し、大振幅の顕著な後続相となって観測される一連の様子が、シミュレーションにより明らかに示された。シミュレートされた波形は、観測された後続相の特徴をよく再現した。さらに、水深を変えて行った差分シミュレーションの結果から、海水を考慮しない場合は固体 - 液体境界波が生成されないため後続相も現れない事、海水の水深は後続相の卓越周期や主位相からの遅延時間に影響する事が示された。

キーワード:誘導波, レイリー波, 境界波, 海中音波, アウターライズ地震